OPTIMAL CONTROL OF THE EASIER MANAGEMENT DUAL-MODE POWER-SPLIT TRANSMISSION

P. AHMADIZADEH and B. MASHADI

†*Automotive Eng. Department, Iran University of Science and Technology, Tehran, IRAN.*
p_ahmadizadeh@iust.ac.ir, b_mashhadi@iust.ac.ir

Abstract - **This paper deals with the optimal control strategy design of the easier management (EM) dual-mode power-split device (PSD) in hybrid electric vehicles (HEV). The EM mechanism provides two modes of operation for the HEV based on the clutches performance. One mode is the input split mode and the other is the compound split mode. Dynamic programming (DP) method is used to find the optimal control strategy including the mode switching and the power split between the power sources while providing the charge sustaining condition. Simulation results show significant improvements of the fuel consumption in comparison to the Toyota Hybrid System (THS), which is a well-known industrialized PSD, and in comparison to the rule-based methods.**

***Keywords*— Dual-Mode, Power-Split Device (PSD), Hybrid Electric Vehicle (HEV), Optimal Control, Dynamic Programming (DP)**

I. INTRODUCTION

It has been clearly proved that hybrid electric vehicles have the potential of reducing fuel consumption and greenhouse emissions. However, proper configuration selection, component sizing and supervisory energy management strategy design are the main factors which affect the final performance and efficiency of an HEV. As it is known, there are three kinds of powertrain configurations in HEVs: series, parallel and power-split. The latter is the most common and interesting layout since it can take the advantage of both parallel and series types and can avoid their drawbacks.

In HEVs, energy management strategy is responsible of power distribution among the powertrain components based on the vehicle demand. There are two kinds of energy management strategies: rule-based and optimization approaches. Rule-based methods are based on the heuristic, intuition and human expertise while optimization methods are based on the analytical or numerical operations during which a cost function is minimized while some constraints are met. These methods are aimed to maximize the fuel economy and the powertrain efficiency.

There are some researches that have studied energy management of HEVs equipping with dual-mode power-split devices. Chen and Hwang (2015) presented a control strategy for a dual-mode power-split HEV by using the fuzzy method. Yunlong *et al*. (2015) designed an intelligent control strategy for energy management of a dual-mode powertrain by using combination of a neural net-work controller and an efficiency model. Xiang *et al.* (2017) proposed an online energy management strategy which uses a velocity predictor and a nonlinear model predictive controller to sustain SOC and to decrease the fuel consumption of a dual-mode power-split transmission. Hong *et al*. (2014) studied a mode shift control algorithm which reduces the torque variations in the driveshaft of a dual-mode power-split HEV by using bond-graph models. Bayrak *et al*. (2014) investigated design of a dual-mode power-split architecture considering a distribution of vehicle weights by using optimal design and control strategies. Cipek *et al*. (2013) analyzed dynamic model of a two-mode power-split HEV using the bond-graph method and proposed a conjugate gradient-based BPTT-like optimal control algorithm as the energy management strategy. Ma *et al*. (2012) introduced a two-mode hybrid transmission for a passenger car and then studied different obtainable modes based on kinematic analysis and max-torque capability.

In this paper, the EM dual-mode power-split transmission, which is designed and introduced by Mashadi and Emadi (2010), is modeled dynamically. The aim is to investigate the best performance of this powertrain in a hybrid electric vehicle in terms of providing higher flexibility and less fuel consumption by using the dynamic programming method as the optimal energy management strategy, which is mostly used as a benchmark for evaluating other control strategies. In this way, the system efficacy is studied and compared with the commercialized Toyota Hybrid System as one of the most successful hybrid electric systems in the market. The remainder of this paper is organized as follows: Section 2 provides the HEV modeling during which the dual-mode power-split mechanism as well as other powertrain components are introduced and modeled. Section 3 analyzes the power flow of this dual-mode system. Section 4 reviews the basic concepts of dynamic programming and then formulizes the optimal control problem for the considered HEV. Section 5 presents and discusses the optimal control results of the introduced transmission and finally, the paper is concluded in Section 6.

II. HEV MODELING

A. Powertrain Description

Overall layout of the studied dual-mode power-split powertrain is shown in Fig. 1. This hybrid transmission system consists of a compound planetary gear (CPG), two motor-generators (MGs) and two clutches (CL1 and CL2). The CPG has four nodes: the ring gear (R), the carrier gear (C), the front sun gear (S_f) and the rear sun gear (S_r). C is connected to the engine, S_r is connected to MG1 and R is connected to the output; connection of MG2 depends on the clutches performance. In mode 1, where CL1 is open and CL2 is closed, the system operates in the input split mode and the MG2 is connected to the output, directly. In mode 2, where CL1 is closed and CL2 is open, the system works in the compound split mode and the MG2 is interrelated by the PSD.

Figure 2 shows bar diagram of the dual-mode PSD in mode 1. The complete set of dynamic equations of this mode is:

$$\dot{\omega}_e I_e = T_e - F_r.(R+S_r)\,, \tag{1}$$

$$\dot{\omega}_{MG1} I_{MG1} = F_r.S_r + T_{MG1}\,, \tag{2}$$

$$\dot{\omega}_{out}(I_{MG2} + \frac{R_{tire}^2}{K^2}M) = T_{MG2} + F_r.R - \frac{T_{load}}{K}\,. \tag{3}$$

Equation (1) includes dynamics of the engine where I_e is the engine inertia, T_e is the engine torque, ω_e is the engine's rotational speed, R and S_r are the radii of the ring and rear sun gears, respectively, and F_r is the internal reaction force between the rear planet pinions and every node of the CPG. Equation (2) shows dynamics of the MG1 where I_{MG1} is the inertia of MG1, ω_{MG1} is the MG1 speed and T_{MG1} is the MG1 torque. Equation (3) represents dynamics of the vehicle and MG2 where ω_{out} is the output shaft speed which is equal to the speed of MG2, I_{MG2} is the inertia of MG2, T_{MG2} is the MG2 torque, R_{tire} is the tire radius, K is the final drive ratio, M is the vehicle mass, T_{load} is the road's resistive torque and is calculated based on Eq. (4). It should be noted that the gears inertia are not included in Eqs. (1)-(3) and are ignored due to being small in comparison to inertias of the power sources. Therefore, since there is no power source connection to the S_f, the internal force of the front sun can be considered as zero.

$$T_{load} = (0.5\rho C_D A_f v^2 + mg\sin\theta + f_r mg\cos\theta)R_{tire} + T_f\,. \tag{4}$$

where ρ is the air density, C_D is the drag coefficient, A_f is the frontal area, v is the vehicle velocity, m is the vehicle mass, g is the gravitational acceleration, θ is the slope angle, f_r is the rolling resistance coefficient and T_f is the brake torque applied by the friction brake system.

Kinematic constraint of this mode can be stated as follows:

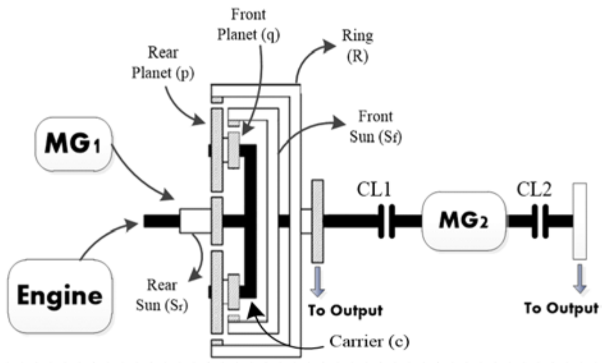

Fig. 1: Dual-mode PSD (Mashadi and Emadi, 2010)

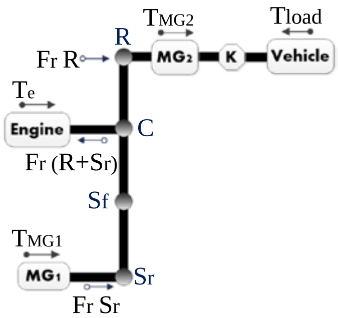

Fig. 2: Bar diagram of mode 1

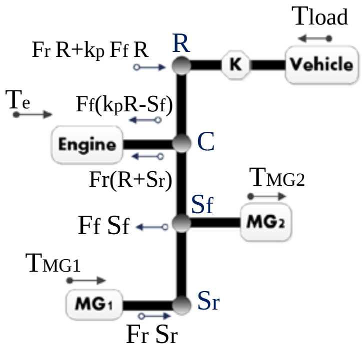

Fig. 3: bar diagram of mode 2

$$(R+S_r)\dot{\omega}_e = R\dot{\omega}_{out} + S_r\dot{\omega}_{MG1}\,. \tag{5}$$

Combining Eqs. (1)-(5) in a matrix format results in

$$\begin{bmatrix} I_e & 0 & 0 & R+S_r \\ 0 & I_{MG2}+(\frac{R_{tire}}{K})^2 M & 0 & -R \\ 0 & 0 & I_{MG1} & -S_r \\ R+S_r & -R & -S_r & 0 \end{bmatrix} \begin{bmatrix} \dot{\omega}_e \\ \dot{\omega}_{out} \\ \dot{\omega}_{MG1} \\ F_r \end{bmatrix} = \begin{bmatrix} T_e \\ T_{MG2} - \frac{T_{load}}{K} \\ T_{MG1} \\ 0 \end{bmatrix}. \tag{6}$$

Figure 3 illustrates the bar diagram of mode 2 and by following the same procedure, the matrix format of this mode can be obtained as

$$\begin{bmatrix} I_e & 0 & 0 & 0 & R+S_r & k_pR-S_f \\ 0 & (\frac{R_{tire}}{K})^2 M & 0 & 0 & -R & -k_pR \\ 0 & 0 & I_{MG1} & 0 & -S_r & 0 \\ 0 & 0 & 0 & I_{MG2} & 0 & S_f \\ R+S_r & -R & -S_r & 0 & 0 & 0 \\ k_pR-S_f & -k_pR & 0 & S_f & 0 & 0 \end{bmatrix} \begin{bmatrix} \dot{\omega}_e \\ \dot{\omega}_{out} \\ \dot{\omega}_{MG1} \\ \dot{\omega}_{MG2} \\ F_r \\ F_f \end{bmatrix} = \begin{bmatrix} T_e \\ -\frac{T_{load}}{K} \\ T_{MG1} \\ T_{MG2} \\ 0 \\ 0 \end{bmatrix}. \tag{7}$$

In Eq. (7), k_p is the ratio of the inner planetary gear radius to the outer planetary gear radius and is defined as:

$$k_p = \frac{q}{p}\,. \tag{8}$$

B. Engine Model

In this HEV, a 1.8 L high-efficient 73 kW internal combustion engine with maximum torque of 142 N.m is used which belongs to the THS-III (Kim *et al*., 2012). Since power, efficiency and fuel consumption are the main focus of the supervisory control problem of HEVs, the engine dynamics and the combustion process can be ignored. Calculation of the fuel consumption can be done based on the BSFC map illustrated in Fig. 4.

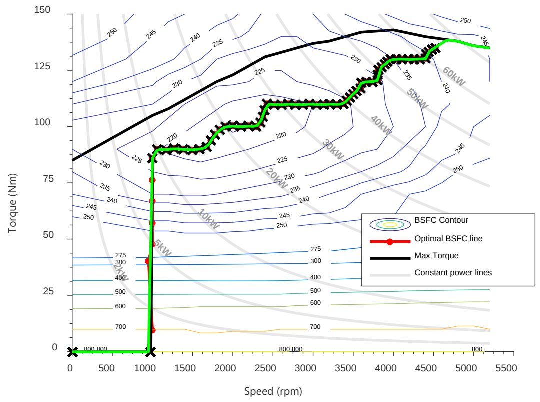

Fig. 4: BSFC map of the THS-III engine

Table 1: Motor/Generator specifications (Kim *et al.*, 2012)

Electric Machine	Parameter	Value
MG1	Max Power	±42 kW
	Max Torque	±140 N.m
MG2	Max Power	±60 kW
	Max Torque	±200 N.m

Table 2: Battery specifications (Hong *et al.*, 2013)

Parameter	Capacity	Nominal Voltage	Max Dis-charge Power	Max Charge Power
Value	6.5 A.hr	201.6 V	25 kW	20 kW

C. Motor/Generator Models

There are two electric machines in this power-split configuration and both can act as either motor or generator. Although both of them can provide the traction power, but MG1 is usually used as the generator and MG2 is used as the motor. MG1 is attached to S_r and can be used for changing the engine speed as well as charging the battery pack by taking power from the engine based on the driving conditions. MG2 is attached to the output in mode 1 and to the PSD in mode 2 and can take part in providing the required traction force or charging the battery when braking. Specifications of the MGs are illustrated in Table 1.

The torque and speed product of an electric machine calculates the mechanical power. Therefore, the electric power can be obtained as:

$$P_{E-MG} = T_{MG}\,\omega_{MG}\,\eta^{k}\,, \tag{9}$$

where η is an efficiency factor and k is the sign of the mechanical power. If the MG is consuming energy (i.e. the power is positive), k=-1 and if the MG is generating energy (i.e. the power is negative), k=1.

D. Battery Pack Model

The considered battery pack in this model is a 1.35 kW.hr Ni-MH one with specifications illustrated in Table 2 (Kim *et al.*, 2012). An internal resistance equivalent circuit model is considered for modeling the state of charge (SOC) dynamics of this battery pack. This model provides the required accuracy of SOC dynamics and is proper enough to be used in an optimization framework. The SOC rate can be represented as:

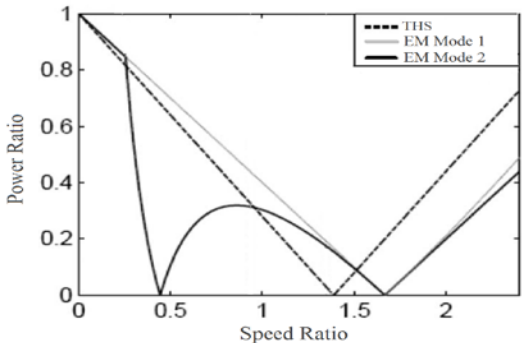

Fig. 5: Power ratio curves for $R/S_r = 1.5$ and $R/S_f = 1.8$

$$S\dot{O}C = -\frac{V-\sqrt{V^{2}-4P_{b}R}}{2R_{i}Q_{pack}}\,, \tag{10}$$

where V is the open circuit voltage, R_i is the internal resistance and Q_{pack} is the battery capacity. The power drawn from or added to the battery pack by the electric machines can be calculated as:

$$P_b = P_{E-MG1} + P_{E-MG2}\,, \tag{11}$$

III. POWER ANALYSIS

In power-split transmissions, the engine power flows to the output through mechanical and electrical paths. In the mechanical path, the power is transmitted directly to the wheels while in the electrical path the power is converted to electricity to charge the battery or to run the electrical machines. Although in the power-split configuration, the engine is decoupled from the wheel and it is allowed to operate in its optimum regions, the power circulation can occur in the electrical path based on the speed ratio and can cause high losses in the transmission system. Toyota Prius HEV shows low efficiency in high speeds due to occurrence of power circulation. Therefore, oversized electric machines are needed to satisfy the power demand (Wang *et al.*, 2014). However, dual-mode power-split devices have the ability to decrease the power circulation and increase the efficiency by adding mechanical points and providing higher flexibility in the transmission operation (Kim *et al.*, 2010).

Power ratio is defined as the power of the electrical path to the engine power. As shown in Fig. 5, the amount of this ratio in the EM dual-mode power-split transmission is less than the THS Prius in most regions which leads to less power circulation. Speed ratio is defined as the output/input speed and at low ratios, the system operates mainly in the first mode while in the mid to high ratios, the system works in the second mode due to having less power ratio. However, it should be mentioned that the energy management controller is responsible to determine the mode of operation at any moment; there may be conditions that less power ratio results in low efficiency of the electric machines according to their operating points and this makes it logical to switch to the other mode (Mashadi and Emadi, 2010).

IV. DESIGN OF ENERGY MANAGEMENT STRATEGY

In this section, an energy management strategy is designed for the HEV equipping with the introduced dual-mode PSD based on the dynamic programming method. DP is a trajectory-based optimization method which is used for finding set of control decisions that leads to a state trajectory in a discrete domain which minimizes some additive cost functions. This method will guarantee a globally optimal solution while some constraints on the states and inputs are met. Here, the aim of dynamic programming is to find the sequence of control decisions at every instant *k* that minimizes the cost function (Jager *et al.*, 2013):

$$J = G_N(x(N)) + \sum_{k=1}^{n} L_k(x(k), u(k), w(k)) . \quad (12)$$

For which

$$x(k+1) = f(x(k), u(k), w(k)) . \quad (13)$$

Subject to

$$x(k) \in X(k) \qquad u(k,x) \in U(k) , \quad (14)$$

where, L is the instantaneous transition cost, G_N is the terminal cost at $k=N$. $x(k)$ is the state vector within the state space $X(k)$, $u(k)$ is the control input vector within the input space $U(x(k),k)$, $w(k)$ is the known disturbance and f represents the system dynamics.

$$g_i(x(k)) \le 0 \qquad i = 1, 2, ..., q , \quad (15)$$

$$h_i(u(k)) \le 0 \qquad i = 1, 2, ..., p . \quad (16)$$

Bellman's Principle of Optimality is used to solve the formulated optimization problem (Bellman, 1957).

A. Application of Dynamic Programming to the HEV

The first step in applying DP to the power management problem of HEVs is to determine which states and control inputs have to be discretized. The complete set of states and inputs of the system described in the previous section are brought in Table 3.

The battery SOC must be discretized since its dynamics are independent from the mechanical states and are directly effective on the control decision of power splitting required at any moment between the internal combustion engine and the battery pack. Similarly and since it is needed to determine the engine status at any moment, the engine speed must be discretized too.

A desired HEV performance will absolutely be provided in case of less fuel consumption. One way to achieve this aim is to make the engine work on the optimum operating line (OOL) which provides the fuel-efficient points at different powers. This can be done in the studied HEV configuration since the engine is not connected directly to the wheels and can work independent of the vehicle speed. Therefore, the engine torque can be obtained by using the engine speed and the OOL of the BSFC map at any moment (Figure 4). It should be noted that limiting the engine to work on the OOL in usual non-hybrid vehicles would decrease drivability characteristics of the vehicle; however, it can be done in our HEV powertrain by using the introduced dual-mode power-split mechanism as well as the electric machines which can compensate the remaining required power.

Table 3: system total states and inputs

States	Inputs
ω_e: engine rotational speed ω_{MG1}: MG1 rotational speed ω_{MG2}: MG2 rotational speed SOC: state of charge	T_e: engine torque T_{MG1}: MG1 torque T_{MG2}: MG2 torque

Table 4: HEV specifications

Parameter	Value
Vehicle mass	1450 kg
Tire radius	0.287 m
Final drive ratio	3.3
Frontal area	2.52 m^2
Aerodynamic drag coefficient	0.28
Rolling resistance coefficient	0.015
Air density	1.2 kg/m^3
Engine inertia	0.18 kg.m^2
MG1 inertia	0.0226 kg.m^2
MG2 inertia	0.0226 kg.m^2

The torque of MG1 or MG2 can be considered as the input. However, since MG1 controls the engine speed and has the ability to charge the battery pack or provide the traction force, its torque is regarded as the input in this paper and is discretized. Thus, other unknown parameters can be calculated using Eqs. (6) and (7) for modes 1 and 2, respectively, according to the HEV's specification provided in Table 4.

Since the driving cycle is considered as a priori in this optimal control method, the speed and acceleration of the output shaft can be obtained as:

$$\omega_{out} = \frac{K}{R_{tire}} v \quad and \quad \dot{\omega}_{out} = \frac{K}{R_{tire}} \dot{v} . \quad (17)$$

Now, considering that ω_e and SOC are meshed as the states and T_{MG1} is meshed as the input, the optimal control problem can be considered according to the following cost function:

$$J = \sum_{k=0}^{N-1} (FC_k + \alpha.\Delta SOC_k + \beta.Mode_k) . \quad (18)$$

Equation (18) includes the fuel consumption (first term), the SOC penalty (second term) which is required for efficient battery usage and the mode penalty (third term) which is needed to prevent excessive switching between the modes. Larger values of α guarantee the SOC to be in the desired window (0.4-0.7) and to converge the final SOC to its initial value at the end of the driving cycle which provides the charge sustaining strategy. Larger values of β lead to less frequent gear shifting, but the larger fuel consumption. α is considered 50000 and β is considered 0.05 in this paper. This problem must be solved while meeting some inequality constraints coming from performance limitations and characteristics of the HEV components. Violation of any constraint leads to consideration of a large penalty cost.

$$\omega_{e,\min} \le \omega_e \le \omega_{e,\max}$$

$$\omega_{MG1,\min} \le \omega_{MG1} \le \omega_{MG1,\max}$$

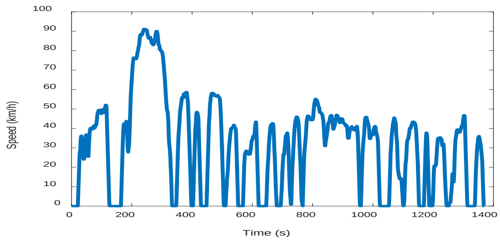

Fig. 6: UDDS driving cycle

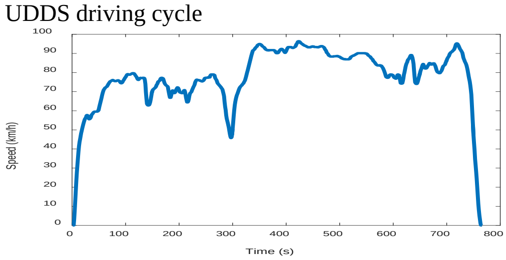

Fig. 7: HWFET driving cycle

$$\begin{aligned}\omega_{MG2,\min} &\le \omega_{MG2} \le \omega_{MG2,\max}\\ SOC_{\min} &\le SOC \le SOC_{\max}\\ T_{MG1,\min} &\le T_{MG1} \le T_{MG1,\max}\\ T_{MG2,\min} &\le T_{MG2} \le T_{MG2,\max}\\ P_{batt,\min} &\le P_{batt} \le P_{batt,\max}\end{aligned} \tag{19}$$

V. SIMULATION RESULTS

In this section, performance of the proposed HEV powertrain will be studied based on the DP based controller as its energy management system. The investigation is done during two common driving cycles: 1) urban dynamometer driving cycle (UDDS). This cycle simulates an urban rout with frequent stops and consists of two phases; the first 505 seconds form the first phase and the other 876 seconds are the second phase. 2) The highway fuel economy test (HWFET) cycle which is a chassis dynamometer driving schedule developed by the US EPA for determination of fuel economy of light duty vehicles. Both driving cycles are shown in Figs. 6 and 7.

Fuel consumption results are shown in Table 6 for the proposed dual-mode power-split transmission and the Toyota Hybrid System (THS) considering two types of controllers: rule-based and DP. The DP controller provides significant improvement in comparison to the rule-based one as per transmission in both driving cycles. This can be related to the global nature of the DP solution which takes the driving cycle as a priori and hence can establish the best performance. Moreover, the EM dual-mode PSD provides less fuel consumption than the THS. This is because of the mode switching ability of the system that enables it to choose the proper operating mode based on the driving conditions which can finally lead to better fuel economy. SOCs of the dual-mode HEV are illustrated in Figs. 8 and 9 for the DP method. As it is desired, the initial and final values of the SOC in both driving cycles are equal, approximately, which demonstrates the charge sustaining condition. This shows that the battery SOC is maintained in an operating range at the end of the driving cycle and the HEV is ready for experiencing further driving conditions.

Table 6: Fuel consumption results (L/100km)

Driving cycle	EM dual-mode (Rule-based)	THS (Rule-based)	EM dual-mode (DP)	THS (DP)
UDDS	4.3	5	2.64	2.88
HWFET	4.78	5.22	3.25	3.38

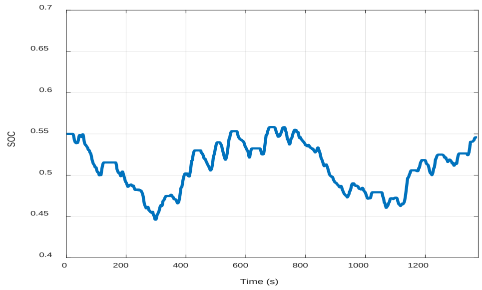

Fig. 8: SOC on UDDS driving cycle

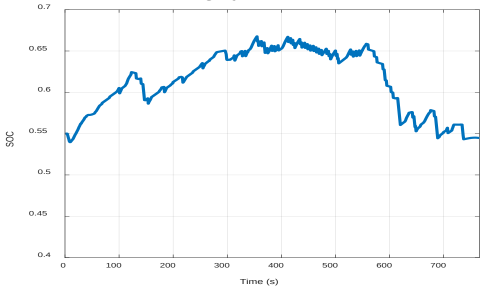

Fig. 9: SOC on HWFET driving cycle

Figures 10 and 11 show the mode changing policy of the DP controller. In low speeds, the dual-mode system is mainly working in mode 1 while in high speeds the main operation is in mode 2. This can be related to the concept of providing less power ratio explained in Section III. In mode 1, power circulation in low speeds is less than high speeds while in mode 2, the contrary happens. This performance leads to better fuel efficiency for the dual-mode system than the THS.

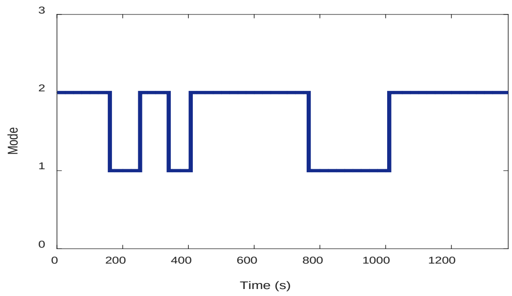

Fig. 9: Operating mode of the mechanism (UDDS)

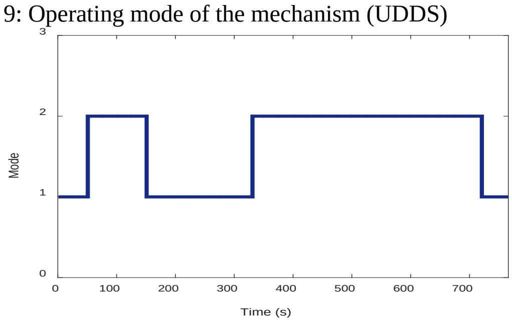

Fig. 11: Operating mode of the mechanism (HWFET)

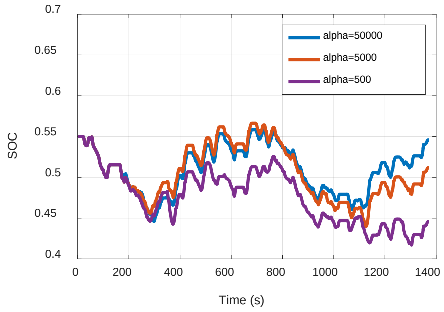

Fig. 12: Effect of changing the coefficient α (UDDS)

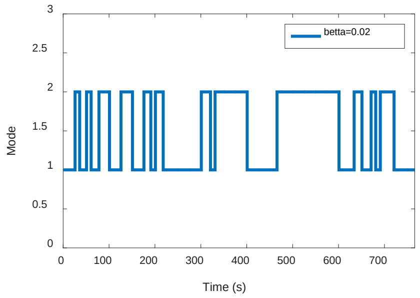

Fig. 13: Effect of changing the coefficient β (HWFET)

Figure 12 shows the effect of changing the coefficient α on the SOC for the UDDS. As can be seen, smaller values of α lead to the final SOC values lower than the initial one. This means that the controller can use more battery charge by considering smaller α; although less fuel consumption can be provided by considering smaller coefficients, but the battery charge tends to deplete at the end of the driving cycle. Figure 13 illustrates the effect of considering smaller value of β on the mode changing policy for the HWFET. Although better fuel economy can be achieved, but the number of mode changings is high which makes it infeasible to be applied practically.

VI. CONCLUSION

In this paper, the EM dual-mode power-split device is introduced and modeled dynamically. The device has the ability of providing two modes of operation for the HEV transmission: input split mode and compound split mode. Based on the power analysis, the HEV is expected to work in mode 1 in low to mid speeds and in mode 2 in high speeds. To exactly determine the best mode of operation which guarantees the minimum fuel consumption while meeting the power demand, an energy management strategy is designed by using the dynamic programming method. Results show significant reduction of the fuel consumption by using this mechanism in the HEV in comparison to the well-known hybrid electric vehicle THS, which is due to the system capability in choosing the most efficient mode of operation considering the driving conditions. Moreover, the charge sustaining strategy is provided for the HEV by having the initial SOC value at the end of the driving cycle. It can be concluded that this dual-mode PSD is capable of being used as the HEV transmission and DP results can be used as a benchmark for designing practical controllers like the rule-based ones.

REFERENCES

Bayrak, A.E., Y. Ren and P.Y. Papalambros, "Optimal dual-mode hybrid electric vehicle powertrain architecture design for a variety of loading scenarios," *Proc. of the ASME Int. Design Eng. Tech. Conf. & Comp. and Inf. in Eng. Conf.*, New York, USA, (2014).

Bellman, R.E., *Dynamic Programming*, Princeton University Press, NJ, (1957).

Chen, J.S. and H.Y. Hwang, "Control Strategy for Two-Mode Hybrid Electric Vehicle by Using Fuzzy Controller," *Int. J. of Comp., Elec., Autom., Cont. and Inf. Eng.*, **9**, 1669-1676 (2015).

Cipek, M., D. Pavković and J. Petrić, "A control-oriented simulation model of a power-split hybrid electric vehicle," *Applied Energy*, **101**, 121-133 (2013).

Hong, S., W. Choi, S. Ahn, Y. Kim and H. Kim, "Mode shift control for a dual-mode power-split-type hybrid electric vehicle," *Proc. IMechE Part D: J. of Automobile Engineering*, **228,** 1217–1231 (2014).

Jager, B.D., T.V. Keulen and J. Kessels, *Optimal control of hybrid vehicles, Advances in Industrial Control*, Springer (2013).

Kim, N., J. Kwon and A. Rousseau, "Trade-off between Multi-mode Powertrain Complexity and Fuel Consumption," *the 25th World Battery, Hybrid and Fuel Cell Electric Vehicle Symposium & Exhibition*, Shenzhen, China (2010).

Kim, N., A. Rousseau and E. Rask, "Vehicle-level control analysis of 2010 Toyota Prius based on test data," *Proceedings of the Institution of Mechanical Engineers, Part D: Journal of Automobile Engineering*, **226**, 1483-1494 (2012).

Ma, X., Y. Zhang and C. Yin, "Kinematic Study and Mode Analysis of a New 2-Mode Hybrid Transmission," *Proc. of the FISITA World Congress*, Beijing, China (2012).

Mashadi, B. and A.M. Emadi, "Dual-mode power-split transmission for hybrid electric vehicles," *IEEE Transaction on Vehicular Technology*, **59**, 3223-3232 (2010).

Wang, W., R. Song, M. Guo and S. Liu, "Analysis on compound-split configuration of power-split hybrid electric vehicle," *Mechanisms and Machine Theory*, **78**, 272-288 (2014).

Xiang, C., F. Ding, W. Wang and W. He, "Energy management of a dual-mode power-split hybrid electric vehicle based on velocity prediction and nonlinear model predictive control," *Applied Energy*, **189**, 640-653 (2017).

Yunlong, Q., W. Weida and X. Changle, "Neural network and efficiency-based control for dual-mode hybrid electric vehicles," *34th Chinese Control Conf.* (2015).

Received: October 11, 2016.
Sent to Subject Editor: November 1, 2016.
Accepted: April 17, 2017.
Recommended by Subject Editor: Fabricio Garelli